A Fundamental Study on Mixture Formation Process in the Combustion Chamber of a Gas Engine

M.Tsue, H.Kakutani, H.Kashiwaya and T.Kadota

Department of Energy Systems Engineering
University of Osaka Prefecture
1-1 Gakuen-cho, Sakai 593
Japan

ABSTRACT

An experimental and theoretical study was carried out of the mixture formation process in the combustion chamber of a gas engine. The planar laser induced fluorescence (PLIF) technique was applied for the visualization of the concentration distribution in the combustion chamber. The fluorescent images were acquired with a CCD camera installed a image intensifier, and they were processed by a image analysis system. A three dimensional numerical analysis was applied for the prediction of the fuel vapor concentration and velocity profile in the combustion chamber. The computational procedure is based on the SIMPLE algorithm. The fuel concentration profile was obtained during the intake stroke in the case that the fuel is injected continuously in the intake port. The effect of the fuel and air mixing behavior in the intake port on the mixture formation process in the combustion chamber was also investigated.

INTRODUCTION

It has widely been recognized that the understanding in-cylinder processes in gas engines is an important factor in improving the thermal efficiency and reducing the exhaust emission of pollutants. Especially, fuel-air mixing process is one of key factors, which has a dominant effect on the ignition process, flame propagation and formation of undesirable pollutants in the combustion chamber of the engine.

Several experimental studies have been made of mixture formation process in the combustion chamber. The fuel concentration has been measured by using the gas sampling method(1-3). The laser Rayleigh scattering method (4-6) has proved to be valuable for measuring the fuel concentration in the combustion chamber. In these works, the application of Rayleigh scattering was limited to the point probing of concentration. Data from single point measurements are often hard to interrupt in terms of mixture formation process in the combustion chamber.

Recently, several studies have been carried out of the two dimensional measurement of species concentration distribution. The planar Rayleigh scattering technique has been applied for the turbulent gas jet (7,8) and internal combustion engines (9). The planar laser induced fluorescence technique (10-12) has been applied for the measurement of fuel concentration profile in the combustion chamber. However, it is not easy to explore the mixture formation process only by experiment because of the complexity of the process. Much more theoretical analysis (13-15) need to be directed on this subject for the thorough understanding of the mixture formation process leading to an optimal mixture distribution.

The present paper consists of the first phase of an experimental and theoretical program designed for providing detailed information about the mixture formation process in the combustion chamber of a gas engine. Among a large variety of laser based diagnostic tool potentially applicable to the remote, nonintrusive of species concentration, the planar laser induced fluorescence technique was selected for the two dimensional measurement of fuel concentration distribution in the combustion chamber in this study. As the fluorescent tracer, biacetyl was used. It has been reported (12) that biacetyl is insensitive quenching, and oxygen quenching cannot significantly conflict with quantitative measurements in the engine. A three-dimensional numerical analysis was also made of the mixture formation process. The measured and predicted results of the fuel concentration profile were obtained during the intake stroke of a motored engine. The comparison between measured and predicted results was made for the examination of the accuracy of the prediction. The effects of state of inlet mixture, on the mixture formation process were also studied.

EXPERIMENTAL PROCEDURE

Figure 1 shows a schematic diagram of the experimental apparatus. Provided in the measurement was air-cooled, four stroke-cycle, single cylinder spark ignition engine. The specification of the engine is shown in Table 1. The original engine was modified to permit the installation of an extended combustion cylinder in order to make the optical access feasible. The details of the modified engine are described later (Fig. 2). The engine was driven by a variable speed electric motor. Experiments were carried out for the engine speed of 100 rpm. A timing disk was installed to detect the engine crank angle. The fresh air was allowed to pass through a flow meter, an air filter and an intake port, and to flow into a combustion chamber.

The fuel nozzle with the inner diameter of 3 mm was fixed at the top portion of the intake port (Fig. 2). Biacetyl was used as the fluorescent tracer. The air supplied by a compressor was allowed to pass though a flow meter and to contact with the liquid biacetyl in the glass cylinder. Thereafter, the air and biacetyl vapor mixture generated in the glass cylinder was injected from the fuel nozzle continuously in the intake port. Since biacetyl has the good vaporization properties relative to other tracers because of its low boiling point of 361 K, less condensation problems were expected. The injection velocity was found to be about 14 m/s.

The light source was the third harmonic (355 nm) of the Nd:YAG laser (Spectra Physics, GCR-11), which was provided 60 mJ of energy in a 5-6 nsec pulse. The beam was formed into a thin sheet 10 mm wide and 0.5 mm thick by use of a convex lens and a cylindrical lens. The fluorescent emission was transmitted through the piston window and

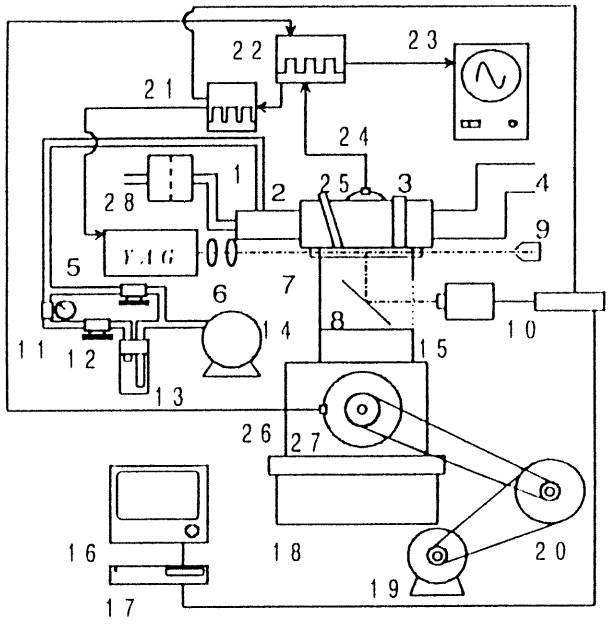

1. Fuel nozzle 2. Intake pipe 3. Cylinder head 4. Exhaust pipe 5. YAG laser 6. Lenses 7. Extended cylinder 8. Mirror 9. Beam trap 10. CCD camera 11. Air flow meter 12. Valve 13. Mess cylinder 14. Compressor 15. Cylinder 16. Monitor 17. Video deck 18. Moving desk 19. Motor 20. Pulley 21, 22. Pulse generator 23. Oscilloscope 24, 26. Photointerrupter 27. Timing disk 28. Air filter

Fig. 1 Experimental apparatus

Table 1 Engine specifications

Type of Engine	Four-stroke-cycle Spark Ignition Engine
Cooling System	Air-cooled
Number of Cylinder	1
Displacement Volume	640 cm^3
Bore x Stroke	95 mm x 90.4 mm
Compression Ratio	9.7(3.5)
Intake Valve Timing	O: 32^0BTDC C: 68^0ABDC
Exhaust Valve Timing	O: 70^0BBDC C: 30^0ATDC
Ignition Timing	0^0BTDC below 220rpm 28^0BTDC above 4300rpm

reflected by the mirror to a CCD camera with an image intensifier. The image intensifier was gated with a trigger pulse, which was simultaneously sent to the laser for the trigger of firing at a specified crank angle. All the equipments comprising the optical detection system were enclosed in a dark box. The images were recorded by the video recorder

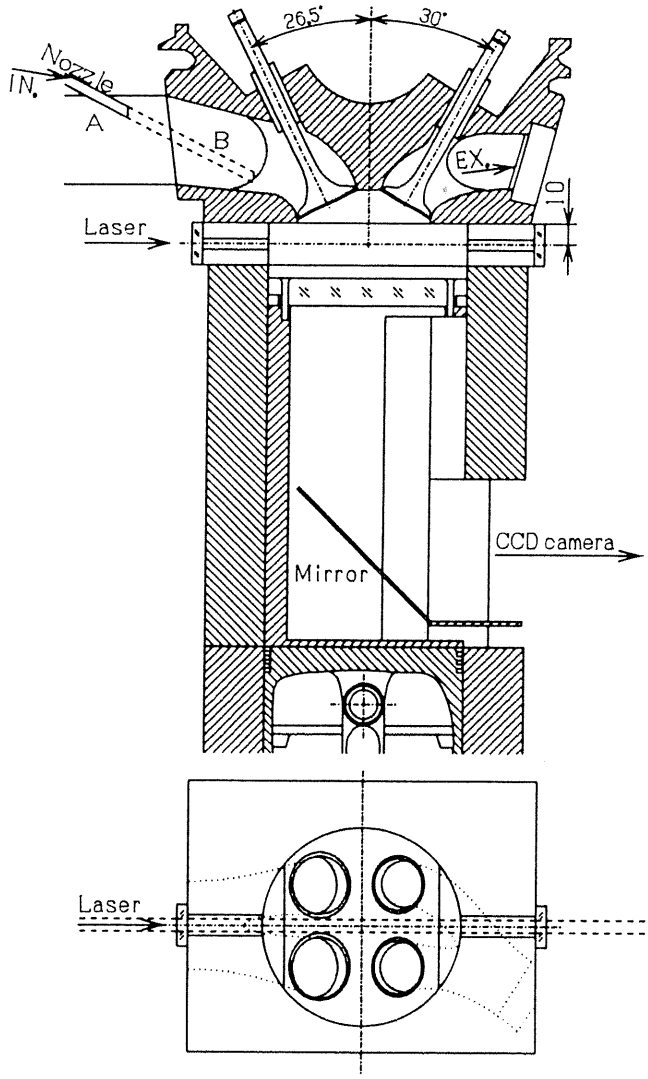

Fig. 2 Detailed geometry of the combustion chamber

and processed by a image analysis system. The background image is subtracted from the source image and the fluorescence intensity was determined. The background images were taken during cycles without fuel injection before the measurements.

Figure 2 shows the detailed geometry of the combustion chamber. The silica windows were installed on the side wall of the extended combustion cylinder which was mounted in the cylinder head and the cylinder of the original engine. An extended piston with a transparent top, which is flat at its tip, was also mounted on the original piston. The compression ratio is set to be 3.5. A mirror was installed inside the piston oriented at 45^0 for the observation through the piston top. The laser sheet was introduced into the cylinder 40 mm below the top of the cylinder head through the silica window. Two kind of nozzles were employed as shown in Fig. 2. The nozzle denoted by A was called here as the long nozzle, the exit of which was located near the intake valve. The nozzle denoted by B was called as the short nozzle.

NUMERICAL ANALYSIS

In order to predict the fuel concentration distribution in the combustion chamber, it is necessary to solve the three-dimensional forms of the partial equations for mass, momentum and the scalar transport. These basic conservation equations in the cylindrical coordinate system have the general

form:

$$\frac{\partial(\rho\phi)}{\partial\rho}+\frac{1}{r}\frac{\partial}{\partial r}(r\rho u\phi-r\Gamma_\phi\frac{\partial\phi}{\partial r})+\frac{1}{r}\frac{\partial}{\partial\theta}(\rho v\phi-\frac{\Gamma_\phi}{r}\frac{\partial\phi}{\partial\theta})+\frac{\partial}{\partial z}(\rho w\phi-\Gamma_\phi\frac{\partial\phi}{\partial z})=S_\phi \quad (1)$$

where: ϕ is a general dependent variable; u, v, and w are fluid velocities in directions r, θ and z, respectively; ρ and Γ_ϕ, S_ϕ are the local density, effective diffusivity and source term. The effects of turbulence are handled by using the familiar k–ε turbulent model. The conservation equations are solved for the eight dependent variables, namely, three component velocities (u, v and w), pressure (p), enthalpy (h), fuel mass fraction (c), turbulent energy (k) and its dissipation rate (ε). The density is obtained via the ideal gas law.

The differential equations are reduced to algebraic form by the control volume method developed by Gosman et al. (16). The fully implicit method and the hybrid method are applied for temporal and spatial differencing schemes, respectively. As a consequence of these practices, the method is computationally stable for arbitrary time step and grid spacing. The algebraic equations are solved iteratively by using the 'SIMPLE' algorithm with Line-by-Line method of TDMA (17).

Figure 3 shows the illustration of the model engine and the coordinate system. The specification of the engine is the same as that of the engine used in the experiment (Table 1). In this analysis, the intake ports are not included in the calculation domain for simplicity. The region in the combustion chamber is divided into small cells by the grids, which expand and contract with the piston motion. The grid division number in r, θ and z direction are 16, 30 and 20, respectively.

The gaseous fuel is injected into the intake port, and the air-fuel mixture flows into the combustion chamber. The velocity and fuel concentration distributions are prescribed around the intake valve as the inlet boundary condition. Figure 4 shows the inflow velocity distribution around the intake valves. The non-uniform distribution without the tangential velocity component is assumed on the basis of the intake port configuration of the engine used in the experiment.

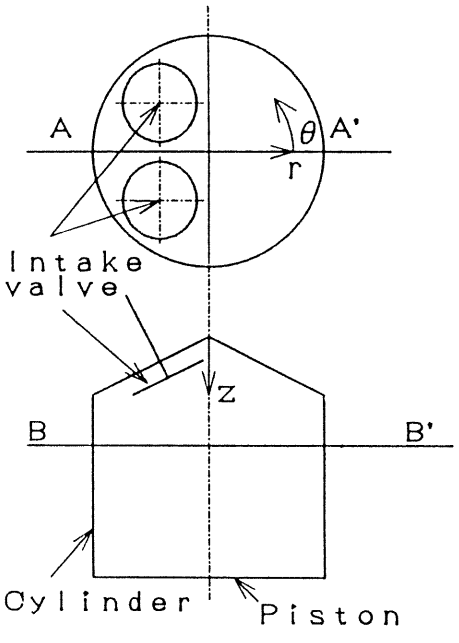

Fig. 3 Illustration of the model engine

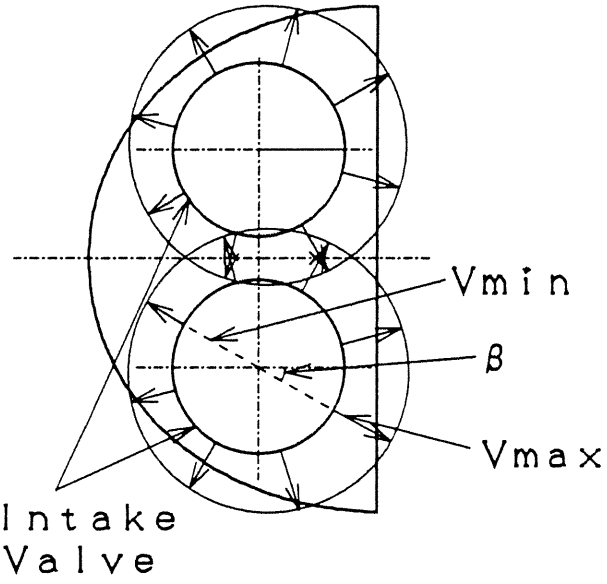

Fig. 4 Inflow velocity distribution

As shown in Fig. 4, the ratio of the maximum velocity V_{max} to the minimum velocity V_{min} is 1.5, and the angle between the maximum velocity direction and the radial direction β is 30^0. The intake valve seat angle is set at 45^0. The fuel concentration distribution is assumed to be uniform around the intake valve. The turbulence kinetic energy of inflow gas k_{in} is set 3 % of the inflow motion kinetic energy. The dissipation rate ε_{in} is given by $\varepsilon_{in} = 2k_{in}^{3/2}/(0.005D)$, where D is bore of the model engine. The temperature of the inflow gas is 288K.

The conventional wall-function method is employed as the boundary condition. The wall temperature is kept constant (373 K). The intake valve moves according to the predetermined lift curve and the valve face is treated as the moving boundary. As to the initial condition at TDC of intake stroke, air in the combustion chamber is assumed to be quiescent, and to be at the atmospheric pressure and room temperature (288 K). Calculation is made from TDC to 180^0 after TDC at every 5^0 crank angles.

RESULTS AND DISCUSSIONS

Measured concentration distribution

Figure 5 shows the fluorescence intensity distributions along the central axis of the incident laser sheet for the short nozzle. They are obtained by averaging images taken at a fixed crank angle for a set of cycles. This ensemble averaging provides the mean fluorescence intensity distribution. The characteristics of the cyclic variation are not described here. Since the nearly linear increase of the fluorescence intensity with the mole fraction of the fluorescent tracer has been reported for the constant temperature and pressure condition (12), it can be considered that fuel concentration distribution is similar to the fluorescence intensity distribution during the intake stroke.

For the short nozzle, it is considered that the fuel and air mixing proceeds in the intake port, and that the nearly uniform mixture flows into the combustion chamber. As shown in Fig. 5(a), at the intake valve side, which is corresponds to the left hand side in the figure, there are two high concentration region, where the inflow mixture formed in the intake port comes directly. The low concentration region appears at the opposite side of the intake valve, although there exists high concentration region in the vicinity of the side wall of the cylinder. The concentration distribution becomes nearly uniform at 180^0 ATDC, although the high concentration

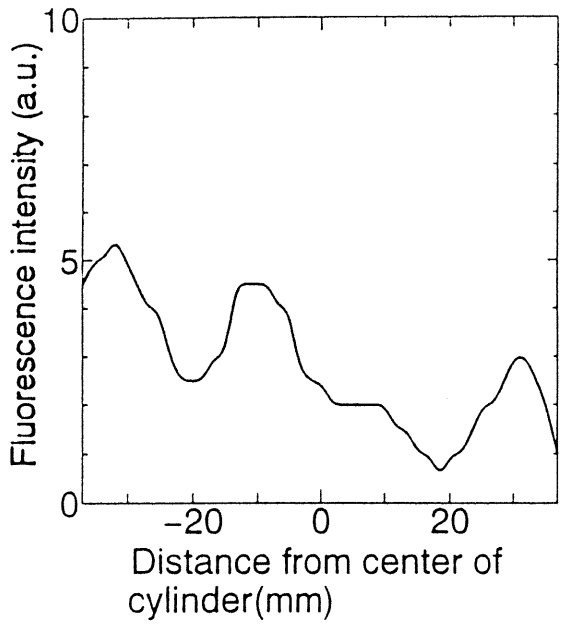

(a) 60^0 ATDC

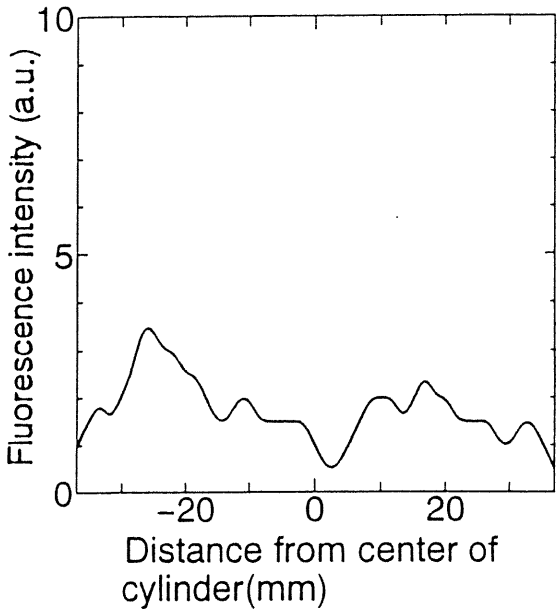

(b) 180^0 ATDC

Fig. 5 Fluorescence intensity distributions along the central axis of the incident laser sheet

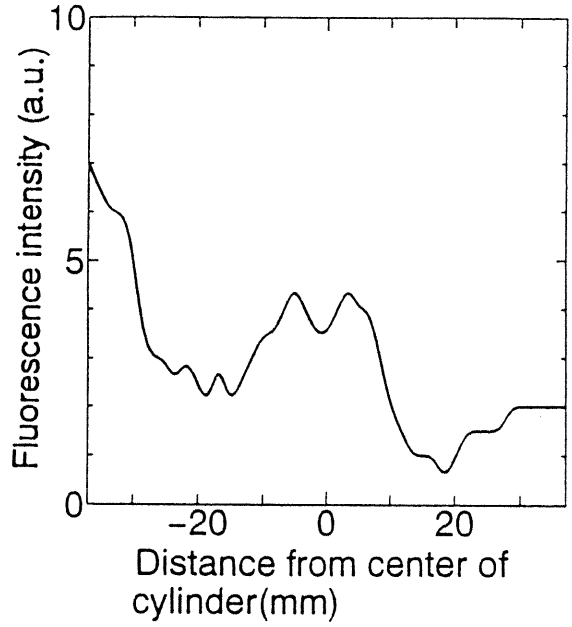

(a) 60^0 ATDC

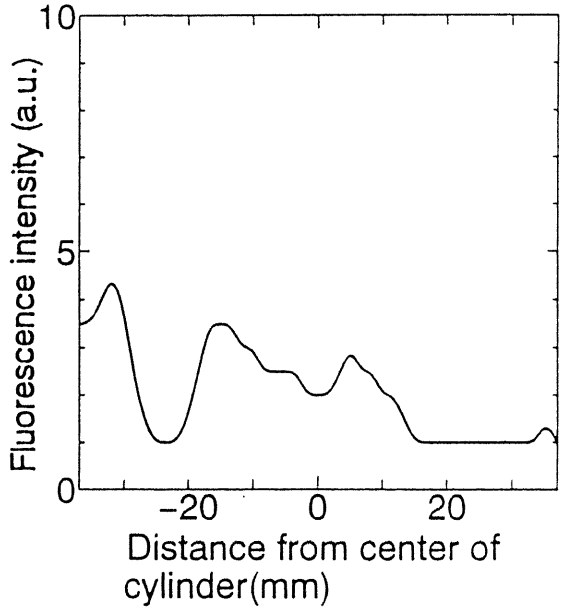

(b) 180^0 ATDC

Fig.6 Fluorescence intensity distributions along the central axis of the incident laser sheet

region exists below the intake valve and the low concentration appears near the center of the combustion chamber (Fig. 5(b)). It seems that the overall concentration is higher in the initial stage of the intake stroke than the last stage of the intake stroke. In the case of continuous injection, the rich mixture forms in the intake port before the intake stroke because of the accumulation of the fuel, and flows into the combustion chamber as the intake valve is opened.

Figure 6 shows the fluorescence intensity distribution for the long nozzle. The fuel concentration is rather high near the cylinder wall at the intake valve side at 60^0 ATDC, as shown in Fig 6(a). For the long nozzle, as the air-fuel mixing is insufficient in the intake port, the concentration distribution of the inflow mixture around the intake valve becomes largely non-uniform. On the basis on the direction of the fuel nozzle as seen in Fig. 2, it is considered that the fuel concentration of the inflow mixture becomes high at the side of the cylinder wall. The high concentration region remains at the intake valve side at the last stage of the intake stroke (Fig. 6(b)). On comparison of the results in Figs. 5 and 6, the time history of the concentration distribution for the long nozzle is similar to that for the short nozzle qualitatively, although the uniformity of the mixture at 180^0 ATDC for the long nozzle becomes less than that for the short nozzle. These results indicate that the fuel and air mixing behavior in the intake port affects the mixture formation process in the combustion chamber.

Calculated results

The fuel concentration and velocity distributions in the combustion chamber were predicted in the case of the short

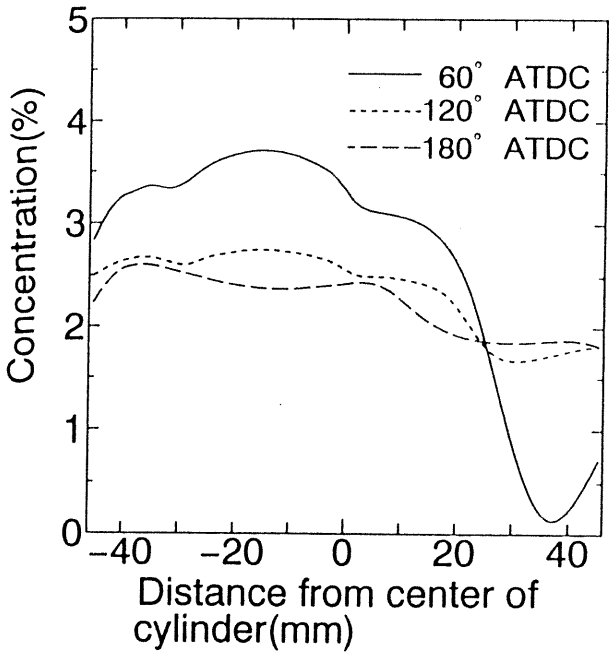

Fig. 7 Predicted concentration distributions

nozzle. The fuel concentration distribution around the intake valve is assumed to be uniform, as mentioned before.

Figure 7 shows the fuel concentration distributions along the same axis as the central axis of the laser sheet for the experiment. At 60^0 ATDC, the high concentration region exists at the intake valve side. At the opposite side of the intake port, there exists high concentration region near the side wall of the cylinder. As the crank angle increases, the concentration at the intake valve side decreases gradually and the concentration at the opposite side of the intake valve increases. Thus, the concentration distribution becomes nearly uniform at the last stage of the intake stroke. As shown in Figs. 5 and 7, it can be concluded that the qualitative agreement between the predicted and measured results for the variation of the concentration distribution with time is satisfactory.

Figure 8 shows the concentration distributions in the r-θ plane including the laser sheet plane (B-B' plane indicated in Fig.3) at 60^0 and 180^0 ATDC. The left hand side of the figure corresponds to the intake valve side. As shown in Fig. 8(a), the high concentration region exists along the side wall of the cylinder at 60^0 ATDC. The maximum concentration region appears at the intake valve side. Figure 8(b) indicates that as the crank angle increases, the fuel concentration at opposite side of the intake valve becomes high gradually and the mixture approaches homogeneity gradually.

Figure 9 shows the velocity distributions in the r-z plane (A-A' plane indicated in Fig. 3) and r-θ plane (B-B' plane) at 60^0 ATDC. The A-A' plane is the r-z plane including the central axis of the laser sheet. The flowfield is represented by arrows whose length is proportional to the projection of the velocity vector into the plane. As shown in Fig. 9(a), the incoming jet flows toward the piston head at the intake valve side. The upward flow is seen at the opposite side of the intake valve. Figure 9(b) indicates clearly that the incoming jet flows along the side wall of the cylinder with a high velocity level, which results in the existence of high concentration region along the side wall of the cylinder, as shown in Fig. 8(a). Thus, it is suggested that this flow plays an important role in the fuel and air mixing process in the combustion chamber.

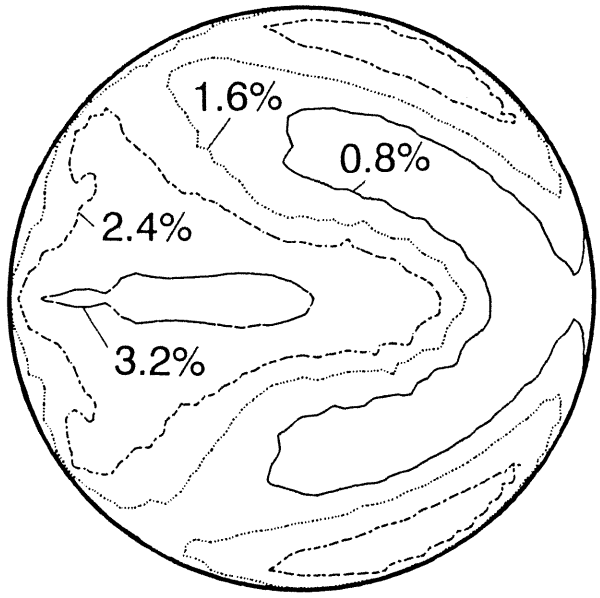

(a) 60^0 ATDC

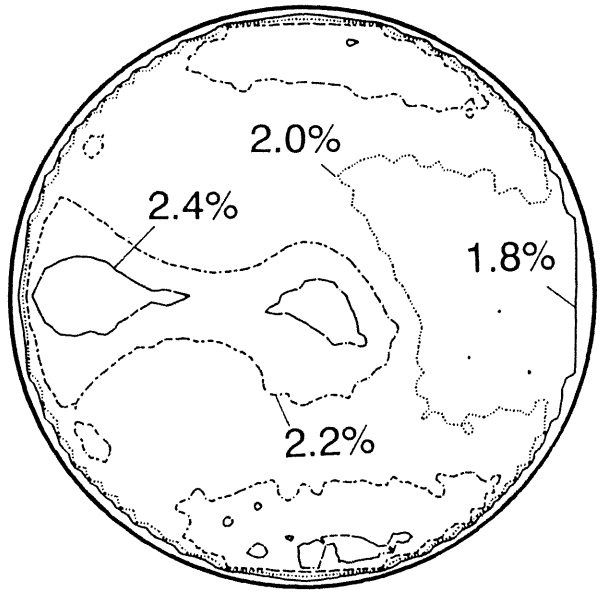

(b) 180^0 ATDC

Fig. 8 Predicted concentration distributions in B-B' plane

CONCLUSIONS

The planar laser induced fluorescence technique was applied for the visualization of the fuel concentration distribution in the combustion chamber of a gas engine. The measurements of the concentration distribution which was caused by continuous injection of the fuel into the intake port of a motored engine were carried out during the intake stroke. In order to explore the effect of state of inlet mixture on the mixture formation process, experiments were carried out for the long and short fuel nozzles. The results showed that in the case that the fuel and air mixing is insufficient in the intake port (long nozzle case), the fuel concentration distribution at the last stage of the intake stroke becomes less uniform. This indicates that the mixture formation process in the combustion chamber is largely affected by the fuel and air

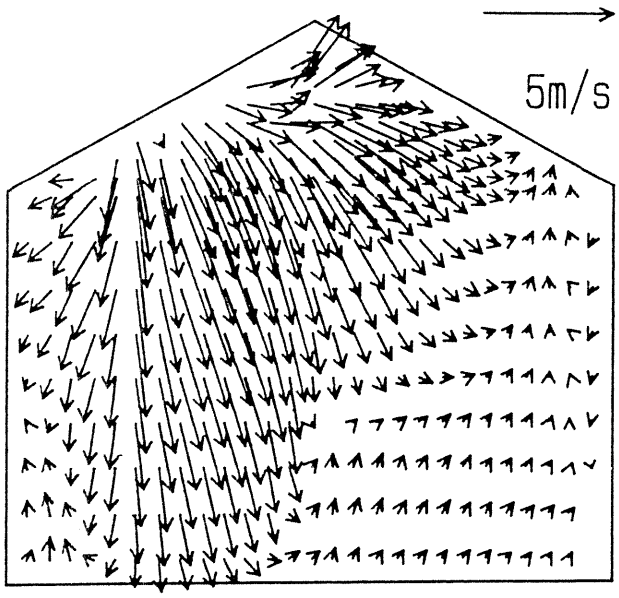

(a) A-A' plane

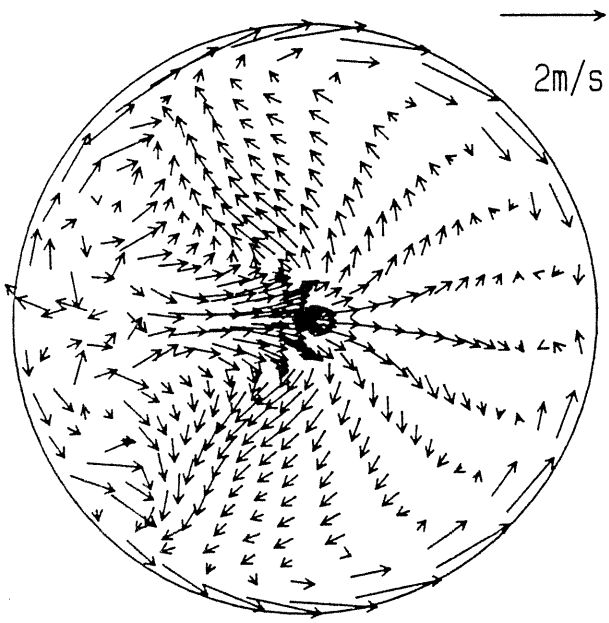

(b) B-B' plane

Fig. 9 Predicted velocity distributions

mixing behavior in the intake port.

Three-dimensional numerical analysis was also applied for the prediction of the time history of the velocity and fuel concentration distributions. The predicted concentration distributions were in qualitatively agreement with the measured results. On the basis of these results, it can be concluded that some success is achieved in predicting the mixture formation process by using the simple numerical analysis in which neither new empirical constants nor new submodels are included.

The laser induced fluorescence technique and the numerical analysis used in this work provides data useful in exploring the mixture formation process in the combustion chamber. Further research remains to be done on the improvement of the accuracy of the measurement. The improvements of the numerical algorithm and the mathematical model including the turbulence model are also needed to obtain the quantitative accuracy of predictions.

ACKNOWLEDGEMENTS

The authors wish to express their gratitude to Suzuki Motor Co., Ltd. for supplying the test equipment.

REFERENCES

1. Ayusawa, T., Nemoto, T., Koo, Y. and Jo, S. H., "Relationship between Local Air-Fuel Ratio and Combustion Characteristics in Spark Ignition Engine", SAE Paper 780147, 1978.
2. Quader, A. A., "The Axially-Stratified-Charge Engine", SAE Paper 820131, 1982.
3. Matsui, K., Tanaka, T. and Ohigashi, S., "Measurement of Local Mixture Strength at Spark Gap of S.I. Engine", SAE Paper 790483, 1979.
4. Kadota, T., "The Application of Laser Rayleigh Scattering to the Local Mixture Strength Measurements in SI Engine during Intake Stroke", SAE Paper 872151, 1987.
5. Kadota, T., Zhao, F. Q. and Miyoshi, K., "Laser Rayleigh Scattering Measurements of the Fuel Vapor Concentration in the Combustion Chamber of SI Engine", The 5th Int. Pacific Conf. Auto. Eng., Beijing, China, November 5-11, 1989.
6. Kadota, T., Zhao, F. Q. and Miyoshi, K., "Rayleigh Scattering Measurements of Transient Fuel Vapor Concentration in a Motored Spark Ignition Engine", SAE Paper 900481, 1990.
7. Escoda, M. C. and Long , M. B., "Rayleigh Scattering Measurements of the Gaseous Concentration Field in Turbulent Jets", AIAA Journal, Vol. 21, No. 1, PP. 81-84, 1983.
8. Tsue, M., Inoue, K., Nakamae, T., Hattori, H. and Kadota, T., "Planar Rayleigh Scattering Method for the Visualization of Concentration Field in a Gaseous Jet", Proceedings of the 2nd JSME-KSME Thermal Engineering Conference, Vol. 2, pp. 453-458, 1992.
9. Zhao, F. Q., Takemoto, T., Nishida, K. and Hiroyasu, H., "Planar Measurements of the Fuel Vapor Concentration in the Combustion Chamber of a Spark Ignition Engine with Laser-Sheet-Induced Rayleigh Scattering", Proceeding of the 10th Internal Combustion Engine Symposium, pp. 307-312, 1992.
10. Lawrenz, W., Kohler, J., Meier, F., Stolz, W., Wirth, R. and Bloss, W. H., "Quantitative 2D LIF Measurements of Air/Fuel Ratios During the Intake Stroke in a Transparent SI Engine", SAE Paper 922320, 1992.
11. Shimizu, R., Matsumoto, S. and Furuno, S., "Measurement of Air-Fuel Mixture Distribution in a Gasoline Engine Using LIEF Technique", SAE Paper 922356, 1992.
12. Baritaud, T. A. and Heinze, T. A., "Gasoline Distribution Measurements with PLIF in a SI Engine", SAE Paper 922355, 1992.
13. Gosman, A. D., Tsui, Y. Y. and Watkins, A. P., "Calculation of Three Dimensional Air Motion in Model Engines", SAE Paper 840229, 1984.
14. Wakisaka, T., Shimamoto, Y. and Isshiki, Y., "Three-Dimensional Numerical Analysis of In-Cylinder Flows in Reciprocating Engines", SAE Paper 860464, 1986.
15. Watkins, A. P., Kanellakopoulos, P. and Lea, C. J., "An Assessment of Discretisation Schemes and Turbulence Models for In-Cylinder Flows", Int. Symposium COMODIA, pp. 499-504, 1990.
16. Gosman, A. D and Ideriah, F. J. K., "TEACH-T: A Computer Program for the Calculation of Two-Dimensional (Plane or Axisymmetrical) Turbulent Reciprocating Flows", Mech. Engrg. Dept. Report, Imperial College of Science and Technology, 1976.
17. Patankar, S. V., Numerical Heat Transfer and Fluid Flow, McGraw-Hill, 1980.